A survey on skeletonization algorithms and their applications ☆

Punam K. Saha [a,b,*], Gunilla Borgefors [c], Gabriella Sanniti di Baja [d,e]

[a] Department of Electrical and Computer Engineering, University of Iowa, Iowa City, IA, USA
[b] Department of Radiology, University of Iowa, Iowa City, IA, USA
[c] Centre for Image Analysis, Uppsala University, Uppsala, Sweden
[d] Institute of Cybernetics "E.Caianiello", CNR, 80078 Pozzuoli, Naples, Italy
[e] Institute for High Performance Computing and Networking, CNR, 80131 Naples, Italy

ARTICLE INFO

ABSTRACT

Skeletonization provides an effective and compact representation of objects, which is useful for object description, retrieval, manipulation, matching, registration, tracking, recognition, and compression. It also facilitates efficient assessment of local object properties, e.g., scale, orientation, topology, etc. Several computational approaches are available in literature toward extracting the skeleton of an object, some of which are widely different in terms of their principles. In this paper, we present a comprehensive and concise survey of different skeletonization algorithms and discuss their principles, challenges, and benefits. Topology preservation, parallelization, and multi-scale skeletonization approaches are discussed. Finally, various applications of skeletonization are reviewed and the fundamental challenges of assessing the performance of different skeletonization algorithms are discussed.

© 2015 Published by Elsevier B.V.

1. Introduction

Skeletonization provides an effective and compact representation of an image object by reducing its dimensionality to a "medial axis" or "skeleton" while preserving the topologic and geometric properties of the object. In two dimensions (2-D), an object is reduced to a curve skeleton consisting of one-dimensional (1-D) structures. In three dimensions (3-D), an object may be converted to a surface skeleton, i.e., a union of 1-D and 2-D structures, or, it may be reduced to a curve skeleton consisting of only 1-D structures. Blum [24] established the foundation of skeletonization in the form of medial loci of an object in R^n that forms the skeleton of the object. This skeleton consists of planes/axes of symmetry with lower dimensionality. The skeleton is useful for object description, retrieval, manipulation, matching, registration, tracking, recognition, compression, and it also facilitates efficient assessment of local object properties, e.g., scale, orientation, topology etc. Analytically, Blum's skeleton, or medial axis, is defined using a grassfire transform process [25] where the object is assumed to be a field of dry grass and a fire is simultaneously lit at all boundary points. The fire propagates inside the object at a uniform velocity.

The skeleton is the set of quench points, where two independent fire-fronts meet [64,84,85,96,165,173,175].

Blum's grassfire transform was later generalized and adopted by the image processing, computer vision, and graphics community in the form of the medial axis, or skeleton, of objects. Commonly, when the *continuous* approach is taken, the boundary of the object is approximated by a polygon or a curve, the grassfire propagation process is realized by curve evolution or constrained mathematical morphological erosion and the skeleton is formed at quench points where the curve evolution process is interrupted [84,85,96,173]. Several researchers have sought geometric features, e.g., the Voronoi diagram, to identify symmetry structures in an object [36,125,128,129]. *Digital* approaches can simulate the grassfire propagation using an iterative constrained erosion process [92,95,126,135,158,190]. Another group of digital skeletonization algorithms [4,7,23,33,145,165] locate maximal balls [165] on digital distance transform field [27].

Blum inspired the representation of an object by the loci of the centers of its maximal inscribed balls (MIBs), together with their radii, which allows exact reconstruction of the object from its medial loci. Computationally, a skeleton may be perceived in three ways: the Blum's quench points by opposing fire-fronts, the centers of MIBs, or the centers of the enclosed balls that touch the object boundary at two or more disjoint locations. For objects in R^2 or R^3, these three skeletonization approaches are roughly equivalent. However, the same is not true for a digital object and these three definitions may produce different skeletons [175]. The inherent discrete nature of digital objects further complicates the skeletonization task by

posing major hurdles, e.g., high sensitivity to small details on the object boundary, homotopy, non-standard definitions of digital balls, etc. Note that high sensitivity to small details on the object boundaries is also featured by non-discrete or continuous approaches to skeletonization [10,118]. In most applications, it is desired that the computed skeleton of a digital object is robust under different conditions of digitization and imaging artifacts; consist of one-voxel thin curves and surfaces to enable tracking; and allow acceptable reconstruction of the original object. This makes the evaluation of the performance of digital skeletonization algorithms challenging [176,177]. Note that taking the continuous route does not remove these problems–the digital object in an image then has to be converted to continuous data and the resulting skeleton may have to be digitized. Neither is trivial.

As discussed above, several computational approaches have been reported in literature toward extracting the skeleton of an object, some of which are widely different in terms of their principles. Several researchers have used continuous methods while others have used purely digital approaches to compute the skeleton of an object. Discussion on different principles of skeletonization algorithms has been reported [175]. In this paper, we present a concise survey of different skeletonization approaches and algorithms and discuss their principles, challenges, and advantages. Also, topology preservation, parallelization, and multi-scale skeletonization approaches are discussed. Finally, various applications of skeletonization are reviewed and the fundamental challenges of assessing the performance of different skeletonization algorithms are discussed.

2. Different approaches of skeletonization

Skeletonization algorithms may be grouped into three major categories based on their principles and the underlying object representation:

(1) Algorithms based on Voronoi diagram or continuous geometric approaches of point clouds, polygonal, or polyhedral representations of object boundaries. Such algorithms use Voronoi edges or planes to construct the symmetry structures or the skeleton.
(2) Algorithms based on the principle of continuous evolution of object boundary-curves where the skeleton is formed at the locations of singularities, e.g., at collision points of opposing boundaries.
(3) Algorithms based on the principle of digital morphological erosion or location of singularities on a digital distance transform (DT) field, e.g., maximal included balls.

Besides the above three categories, Pizer and coworkers [59,122,139] presented algorithms to extract zoom-invariant cores from intensity images. The medial cores are defined as generalized maxima in scale-space produced by a medial filter that is invariant to translation, rotation, and, in particular, zoom. Lantuejoul [94] introduced a mathematical morphological approach for skeletonization using influence zones. Maragos and Schafer [116] used mathematical morphological set operations to transform a discrete binary image using parts of its skeleton containing complete information about its shape and size. See [117,118,170] for early works on mathematical morphological approaches to homotopic thinning in continuous and discrete spaces. Skeletal subsets produced by such methods are dependent on structure elements used for mathematical morphology operations. Also, the resulting skeletons may not preserve connectedness.

It may be noted that most digital approaches to skeletonization use the object representations in pixel (in 2-D) or voxel (in 3-D) grids. A major drawback with such skeletonization algorithms is that these methods may not guarantee single-pixel (or voxel) thin skeletons for all objects, especially, at busy junctions; see Fig. 1. In other words, if
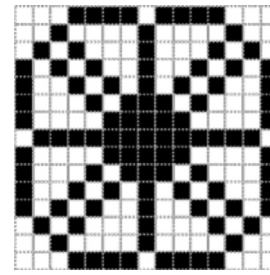

Fig. 1. An example of a busy junction of digital lines forming a diamond-shaped region in 2-D, which may not be thinned any further as the removal of any pixel from the object alters its topology. Note that it is possible to generalize a similar example in 3-D where the junction forms a volume that cannot be thinned.

the object of Fig. 1 or its 3-D version is used as an input, pixel- or voxel-based methods may not remove any pixel or voxel and thus fails to produce a one-pixel thin skeleton. Note that the example of Fig. 1 may be modified to increase the size of the central blobby region. A more complex, but also richer, approach to the object representation is using simplicial or cubical complex frameworks [40,47,50,54,88,98]. The above problem disappears when skeletonizing objects in these frameworks [50,54,98]. In the rest of this section, a brief survey of skeletonization algorithms for each of the above three categories is presented.

2.1. Continuous geometric approaches

Several algorithms [36,128,129] focus on geometric properties of Blum's medial symmetry axis to locate the skeleton of an object. These methods are generally applied on a mesh representation of the object, or on a point-cloud generated by sampling the object boundary. One popular approach under this category is based on the principle of the Voronoi diagram [3,36,125,128,129,185]. The Voronoi skeleton of a polygonal shape is obtained by computing the Voronoi diagram of its boundary vertices and then taking its intersection with the polygonal shape. It may be noted that each additional vertex on the polygon adds a new skeletal branch. Thus, a proper polygonal approximation of a shape is crucial to generate the desired complexity of the skeleton. On the other hand, an accurate polygonal representation of a shape requires a large number of vertices. Thus, in general, Voronoi skeletonization produces a large number of spurious skeletal branches that are not essential for overall representation of the shape. Ogniewicz and Ilg [128] observed that *the skeletal segments, which lie deeply inside the polygonal shape are less sensitive to small changes on the boundary*. Such segments are essential for the description of the global topology and geometry of an object. Based on this observation, they derived different *residual function*s and used those to differentiate spurious branches from those essential to represent the object topology and geometry. Schmitt [167] proved that, as the number of generating boundary points increases, the *Voronoi diagram converges in the limit to the continuous medial locus*, with the exception of the edges generated by neighboring pairs of boundary points. Later, Voronoi skeletonization was generalized for 3-D polyhedral solids [3,11,52,172]. Amenta et al. [3] characterized *inner* and *outer Voronoi ball*s for a set of boundary sample points to reconstruct its power crust, an approximation of a polyhedral boundary, and to compute its Voronoi skeleton. Jalba et al. [80] developed a *GPU-based efficient framework* for extracting surface and curve skeletons from large meshes. Bucksch and Lindenbergh [38] presented a *graph-based approach* to extract the skeletal tree from point clouds using collapsing and merging procedures in octree-graphs. This approach offers a computationally efficient solution for computing skeletons from point clouds that is robust to varying point density and the complexity of the skeleton may be adjusted by varying the size of the octree cell.

Ma et al. [112] introduced a *nearest neighbor approach* to skeletonization from points sampled on the object boundary where each point is associated with a normal vector. For each sample point, the method finds its maximal tangent ball, containing no other sample point, by iteratively reducing its radius using nearest neighbor queries. They showed that the computed skeleton converges to the true skeleton as the sampling density tends to infinity.

2.2. Continuous curve propagation approaches

Some researchers have simulated Blum's grassfire propagation using a *curve propagation model* [84,85,96,142,173]. A thorough review of continuous approaches for skeletonization, together with several discrete skeletonization algorithms from distance transforms, was presented in a book edited by Siddiqi and Pizer [175]. Unlike a morphological erosion approach, such curve evolution processes are modelled using partial differential equations. In the process of continuous curve evolution, certain singularities occur which are mathematically referred to as *shocks* and used to define the skeleton. Leymarie and Levine [96] modeled the curve evolution using an *active contour* on a distance surface and used the singularities of curvature features to initiate skeletal branches. Kimmel et al. [85] segmented the object boundary at singularities of maximal positive curvature and computed a DT from each boundary segment. Finally, the skeleton is located at the *zero level sets* of distance map differences. Siddiqi et al. [173] proposed a Hamiltonian formulation of curve evolution and computed the outward flux of the vector field of the underlying system using the *Hamilton-Jacobi equation*. Skeletons are located at singularities of this flux field. Additionally, they imposed the topology preservation constraints of digital grids to ensure the robustness of computed skeletons.

Using the principle of continuous front propagation for skeletonization, several algorithms [2,9,49,74,186] have focused on *general fields* for front propagation which are smoother than distance transforms and used such fields to impose smoothness on extracted skeletons. Ahuja and Chuang [2] used a *potential field* model where the object border is assigned with constant electric charges and the valleys of the resulting potential field are used to extract the skeleton. Tari et al. [186] used an *edge-strength function* to extract the object skeletons, which equals '1' along the object boundary and elsewhere it is computed using a linear diffusion equation. In this approach, the skeleton is defined as the projection of the singular lines on the elevated surface representation of the edge-strength function and by analyzing the geometry of the level curve of the function. A major advantage of this approach is that the method can be applied to gray scale images as the computation of the edge-strength function only requires the object edge points instead of a complete connected object boundary. Aslan et al. [9] further improved this skeletonization strategy and introduced the notion of *absolute scale* related to the maximum regularization while allowing morphological analysis. An important factor for these algorithms [9,186] is that the resulting skeletons may not be topologically connected. However, such algorithms allow multi-scale regularization of the smoothness of the skeleton. Cornea et al. [49] developed a curve skeletonization algorithm using a *force vector field* while Hassouna and Farag [74] designed a curve skeletonization algorithm using the *gradient vector flow*.

2.3. Digital approaches

The most primitive, yet popular, skeletonization approach is based on simulating Blum's grassfire propagation in a digital grid as an iterative erosion under certain digital topologic and geometric rules. The literature of iterative digital erosion algorithms for skeletonization in 2-D had matured in the early 1990s [92]; however, the same was not true for 3-D skeletonization algorithms. Tsao and Fu [190] reported the first complete 3-D skeletonization algorithm. In terms of computational efficiency, skeletonization algorithms may be classified into sequential [4,7,23,33,95,145] and parallel [17,103,104,108–111,126,135,160,190] algorithms. Digital skeletonization algorithms may be also classified into three categories – (1) fully predicate-kernel based iterative algorithms [95,103,104,126,135], (2) iterative boundary peeling algorithms under topologic and geometric constraints [95,160,190]; and (3) distance transform [26,27,29,30] or DT-based algorithms [4,7,33,145]. Although, fully kernel based skeletonization was established in 2-D during 1980s [92], the first kernel based 3-D skeletonization algorithm was reported by Palágyi and Kuba [135], which was further improved by Németh et al. [126]. In a kernel based approach, topologic and geometric constraints are coupled together. Saha et al. [160] presented an iterative boundary peeling algorithm for 3-D skeletonization where topologic and geometric issues are addressed independently. Others have used distance transforms for skeletonization [4,7,23,33,145,165]. Arcelli and Sanniti di Baja [4] introduced the notion of DT-based skeletonization in 2-D and discussed its advantages. Borgefors et al. [32–34] applied the DT for skeletonization in 3-D. Saito and Toriwaki [164] introduced the idea of using the DT to define the sequence of voxel erosion which has further been studied by other research groups [7,145]. DT based approaches do not require repetitive image scans. Moreover, they do not require to manage two buffers, respectively storing the elements of the current boundary and their neighbors that will constitute the successive boundary. Thus, DT based approaches are characterized by computation efficiency. Also, a DT-driven voxel erosion strategy, together with a suitable choice of distance metric [29] makes the skeletons more robust under image rotation. However, an apparent difficulty of this approach is that it may be hard to parallelize such algorithms. Lantuejoul [94] and Chatzis and Pitas [43] applied mathematical morphology approaches to skeletonization. Several algorithms [71,179,194,197] have been tailored for elongated structures which directly generate curve skeletons for volumetric objects. Even though a few works on gray-scale and fuzzy skeletonization have been presented in literature [171,186,200], the fundamental issues and a comprehensive skeletonization algorithm for fuzzy digital objects have been reported only recently [81]. A DT-driven 3-D skeletonization algorithm [7,81,163] is briefly outlined in the following, which, in principle, is applicable to both binary and fuzzy digital objects:

Primary skeletonization

- locate quench voxels
- filter quench voxels with high local shape significance factor and preserve those in the decreasing order of their DT values
- sequentially delete simple points (see Section 3) not necessary for topology preservation in the increasing order of their DT values

Final skeletonization

- convert two-voxel thick structures into single-voxel thick structures
- remove voxels with conflicting topological and geometric properties

Skeleton pruning

- remove noisy or spurious branches using some measure of global shape significance factor.

The notion of primary and final skeletonization was simultaneously introduced by Saha et al. [157,160] and Sanniti di Baja [165]. Saha et al. defined the two steps for 3-D skeletonization using an iterative boundary erosion approach while Sanniti di Baja presented the idea in 2-D using a DT-based mechanism. Primary skeletonization produces a "thin set" [4] representing the medial axis of the object, where every voxel has at least one background neighbor except at very busy intersections of surfaces and curves where some voxels may be internal voxels, see Fig. 1. A scan-independent choice of quench voxels always produces two-voxel thick skeletons where
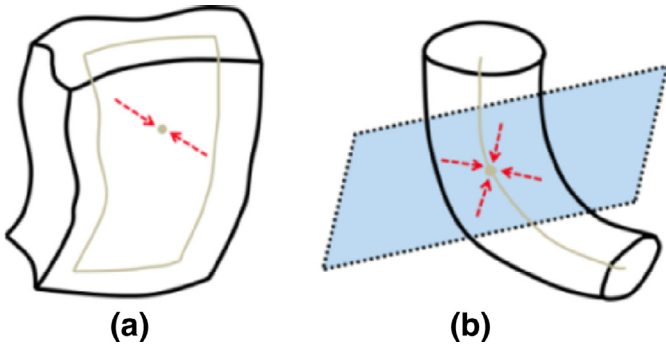
Fig. 2. Illustration of independent fire-fronts meeting at surface (a) and curve (b) quench voxels.

the object has a thickness of an even number of voxels. The primary skeleton thus needs to be further eroded during final skeletonization to generate one-voxel thick skeletons.

Arcelli and Sanniti di Baja [5] introduced a criterion to detect the centers of maximal balls (CMBs) in a 3×3 weighted distance transform, and Borgefors [28] extended it to 5×5 weighted distances. The concept was generalized to fuzzy sets by Saha and Wehrli [161], Svensson [183], and Jin and Saha [81]. A voxel $p \in Z^3$, where Z is the set of integers and Z^3 represents a cubic image grid, is a *fuzzy center of maximal ball* (*fCMB*) or a *fuzzy quench voxel* in a fuzzy digital object $\mathcal{O}$ if the following inequality holds for every neighbor q of p

$$FDT(q) - FDT(p) < \frac{1}{2} \left(\mu_{\mathcal{O}}(p) + \mu_{\mathcal{O}}(q) \right) |p - q|,$$

where FDT is the fuzzy distance transform [162]. The CMBs, or quench voxels, form ridges on the DT map. In other words, a quench voxel cannot pass the DT value or grassfire propagation from itself to any of its neighboring voxels. Definitions of fuzzy quench voxels and CMBs [5] are equivalent for binary digital objects. Two types of quench

voxels, namely *surface* and *curve quench* voxels, are observed in 3-D [7,81,160] (Fig. 2). A surface quench point is formed when two opposite fire-fronts meet, while a curve quench point is formed when fire-fronts meet from all directions on a plane. Jin and Saha [81] handled these two types of quench voxels differently, when filtering the noisy ones. Svensson et al. [184] suggested to remove redundant CMBs [31] and then to use the minimal set as anchor points for a contour peeling algorithm. Minimizing the set of anchor points makes the primary skeleton much thinner two-pixel/voxel thick structures occur in fewer situations.

During the final skeletonization step, two-voxel thick structures are eroded under topology preservation and some additional geometric constraints [7,160,165] maintaining the overall shape of the skeleton. A few examples of skeletonization results are presented in Fig. 3.

3. Topology preservation

For topology preservation in skeletonization, 2-D or 3-D simple point constraints are applied while eroding each individual pixel or voxel. A pixel/voxel is a *simple point*, if and only if, its binary conversion, i.e., conversion from black to white or vice versa, preserves the object components and cavities (and tunnels in 3-D) in the $3 \times 3 (\times 3)$ neighborhood of the candidate pixel/voxel. A concise characterization of 2-D simple points was established in the early 1970s [77,124,150,151]. A characterization of simple points in 3-D is more complex than in 2-D, primarily, due to the presence of tunnels in 3-D. Tourlakis and Mylopoulos [189] presented a generalized characterization of simple points which applies to any dimension. Morgenthaler [120] presented a characterization of 3-D simple points where the preservation of tunnels was imposed by adding a constraint of Euler characteristic preservation before and after the deletion of the candidate voxel. Lobregt et al. [100] presented an efficient algorithm for 3-D simple point detection based on the Euler characteristic preservation. However, as described by Saha et al. [159], their algorithm
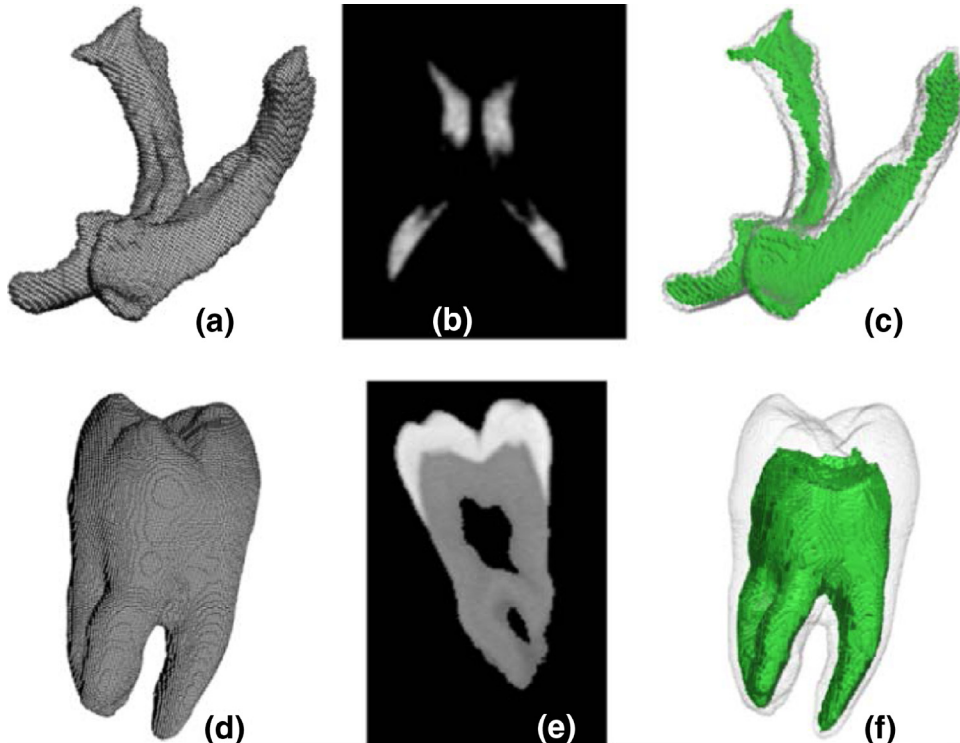

Fig. 3. Results of skeletonization [81] on two anatomic fuzzy structures. (a) A part of the cerebrospinal fluid segmented from a human brain in an MR image. (b) An axial image slice illustrating the fuzziness and noise. (c) Surface rendering of the fuzzy skeleton. (d–f) Same as (a–c) but for micro-CT image data representing a human tooth.

fails to detect the violation of topology preservation when the deletion of a point simultaneously splits an object into two and creates a tunnel. Saha et al. [154,155,157,159] solved this nontrivial challenge of defining the existence or the number of tunnels in the $3 \times 3 \times 3$ *excluded neighborhood* of the candidate voxel, where the central voxel is excluded.

Theorem 1. *If a voxel p has a white 6-neighbor, the number of tunnels $\eta(p)$ in its excluded neighborhood is one less than the number of 6-components of white 18-neighbors of p that contain a 6-neighbor, or, zero otherwise.*

Saha et al. [154,155,157,159] used the above definition of the number of tunnels to formulate a concise characterization of 3-D simple points in the following four-condition format.

Theorem 2. *A voxel p is a (26, 6) simple point in a 3-D binary image if and only if it satisfies the following four conditions.*

Condition 1. *p* has a white (background) 6-neighbor.

Condition 2. *p* has a black (object) 26-neighbor.

Condition 3. The set of black 26-neighbors of *p* is 26-connected.

Condition 4. The set of white 6-neighbors of *p* is 6-connected in the set of white 18-neighbors.

In the above theorem, Condition 1 ensures that no cavity is created by deletion of the point, while Condition 2 confirms that no isolated point is deleted. Condition 3 ensures that, after the deletion of the central point *p*, its neighboring points remain connected. Finally, Condition 4 guarantees that the deletion of a point does not create a tunnel in the neighborhood. Malandain and Bertrand discovered the same result, which was presented in in a two-condition format [22,113]. There is also the possibility of characterizing topology preservation in simplicial and cubical complex frameworks [47,50,88] using the classical notion of homotopy.

4. Parallelization

Almost fifty years ago, Rutovitz [152] proposed the first parallel skeletonization algorithm. Since then, a large number of 2-D parallel skeletonization algorithms have been reported and the first 3-D parallel skeletonization algorithm was presented by Tsao and Fu [190]. The principal challenge in parallel skeletonization emerges from the fact that, although a characterization of simple point guarantees topology preservation when a single simple point is deleted at a time, these characterizations fail to ensure topology preservation when multiple simple points are deleted in parallel. The following strategies have been adopted in the literature to solve this problem of parallel skeletonization.

4.1. Subiterative parallelization scheme

During an iteration, a skeletonization algorithm peels one layer of object voxels while preserving the topology and local elongatedness of the object. In a parallel implementation, one iteration is divided into several subiterations. Two schemes for dividing an iteration in 3-D into subiterations are available in literature – based on the direction of open face(s) of boundary voxels [17,68,95,108,110,123,132,135,190,198] and based on subfield partitioning of the image grid [18,66,111,133,156,160]. In the first scheme, an image is divided into six directional subsets, e.g., north, south, east, west, top, and bottom. One iteration of the skeletonization algorithm is completed in six subiterations, one for each direction, where the voxels in the corresponding directional subset are processed in parallel. In general, directional subdivision cannot eliminate all ambiguous

simple sets and additional restricting conditions are required to ensure topology preservation. Algorithms are available under this category where different numbers of subiterations are used in one complete iteration, e.g., 12-subiteration [103,135], 8-subiteration [134], 6-subiteration [104,132], 3-subiteration [130], and fully parallel [131]. The premise behind the subfield-based parallelization scheme is to divide the image space such that simplicity of any voxel is independent of the object/non-object configuration of any other voxel from the same subfield [66]. Thus, eight subfields are usually defined in the 3-D cubic grid [156,160]. Ma et al. [111] presented a 4-subfield parallel skeletonization algorithm for 3-D cubic grid and established its topology preservation property. Arcelli et al. [6] suggested a 2-subiteration parallel algorithm to compute the surface skeleton of the D⁶ distance transform of a 3-D object without resorting to directional processes.

4.2. Parallelization using minimal non-simple sets

Ronse [148,149] introduced the fundamental notion of minimal non-simple sets in 2-D to study the conditions under which pixels may be removed in parallel while preserving the topology. In particular, he showed that a set of pixels *D* and its proper subsets are all co-deletable in a binary image if each singleton and each pair of 8-adjacent pixels in *D* is co-deletable. Similar results on parallel skeletonization were established by others [62,63,72,107,109] for 2-D, 3-D, and 4-D binary digital images. Such strategies lead to fully parallel skeletonization with topology preservation constraints defined over an extended neighborhood beyond the $3 \times 3 \times 3$ neighborhood needed to characterize singleton simple points. Ma and Sonka [109] presented the first fully parallel skeletonization algorithm in 3-D. Lohou [102] and Wang and Basu [195] detected non-topology preservation and counter examples of Ma and Sonka's algorithm. Lohou [101,102] further studied the non-topology preservation of Ma and Sonka's algorithm and presented an algorithm [106] for automatic correction of Ma and Sonka's algorithm. Recently, Kong [89] extended Ronse's work on minimal non-simple sets to binary images on almost any polytopal complex whose union is the *n*-dimensional Euclidean space, for $n \leq 4$. Passat et al. [137] established a characterization of minimal 3-D simple pairs in the sense that, while each voxel in the pair is independently non-simple, deletion of both voxels leaves the topology of the object unchanged.

4.3. Parallelization using P-simple points:

Bertrand [15,16] introduced a new interpretation of simple points, referred to as *P-simple points*, which guarantees topology preservation even when we delete those points in parallel. A parallel skeletonization scheme based on *P*-simple points uses two steps. In the first step, a set of voxels *D* is identified which may be considered for deletion based on geometric requirements of the skeletonization algorithm. In the second step, the voxels of *D* which are *P*-simple are deleted in parallel. Depending upon the propagation strategy, a parallel skeletonization algorithm using *P*-simple points may be either directional [15,39,103,104,115] or symmetrical [105].

4.4. Parallelization using critical kernels:

Bertrand and Couprie [19–21] designed a new parallel skeletonization scheme for the cubical complex representation of binary digital images using a new notion of "critical kernel of a complex". The parallelization scheme utilizes the following theoretical properties of a critical kernel:

1. Any complex *X* collapses onto its critical kernel.
2. If an essential subcomplex $Y \subset X$ includes the critical kernel of *X*, then *X* collapses onto *Y*.
3. If a subcomplex of *Y* includes the critical kernel of *X* and *Z* is an essential subcomplex of *X* such that $Y \subset Z$, then *Z* collapses onto *Y*.

Bertrand and Couprie [21] proved that the critical kernel is a unifying framework that encompasses parallel thinning approaches using both minimal non-simple set and *P*-simple points. A notion of *constraint set* is introduced into this framework to capture the medial axis during the collapsing process. For example, the constraint set may include the centers of maximal included balls.

5. Multi-scale skeletonization

Blum's medial axis representation produces a unique object description that allows reconstruction of the original object. However, the representation is highly sensitive to small-scale features at the object boundary and, often, it generates medial axes with extremely bushy and complex branches. Multi-scale skeletonization approaches incorporate a regularization or significance factor to control the trade-off between the smoothness and simplicity of the medial axis and representation of object features at target scales. Different principles of multi-scale have been adopted in different skeletonization approaches. Pizer et al. [142] laid out mathematical properties and computational abilities of different approaches and compared and contrasted those.

In Voronoi skeletonization approaches, stability and significance of Voronoi segments are used to reduce spurious branches and to improve the skeleton's robustness. Several significance measures have been proposed in literature [129,185] which are used to establish a hierarchical representation of segments in a Voronoi skeleton. Skeletal segments or branches that are at the periphery of this hierarchy and have a low significance measure are candidates for pruning. This framework underlies the notion of multi-scale skeletons based on the thresholds for hierarchical position and significance of branches. Another perspective of multi-scale skeletonization is to use different regularization levels in terms of initial smoothing of the original object boundary [14,53,141]. At higher levels of smoothing, the skeletons become less detailed and more stable to boundary changes. Essentially, this class of algorithms raises the notion of skeleton scale-space. A different view of multi-scale skeletonization is to use a regularization term, or curve smoothing, during the entire front propagation [69,84,174,186]. Kimia et al. [84] used a regularization approach where a curvature-dependent smoothing component is added to the uniform speed representing the morphological propagation of the fire-front. Tari et al. [186] introduced a blurring radius parameter to control the smoothness of the edge-strength function that in turn decides the smoothness of computed skeletons. This approach leads to simpler and faster implementation applicable to higher dimensions even where there are gaps among object boundary points. Aslan et al. [9] brought the notion of absolute scale to skeletonization by letting the regularization term tend to infinity and dominate the morphological component of curve evolution. Cornea et al. [49] used a different strategy where they computed the divergence of the repulsive force field inside an object by charging the object's boundary and used a threshold on it to model a multi-scale curve skeletonization. Giesen et al. [65] introduced an interesting notion of scale axis transformation that uses a scale multiplicative dilation of maximal included balls along the medial axis of the original object to remove less important features. Miklos et al. [119] applied the discrete scale axis transform to compute multi-scale skeletons from 3-D mesh representation of an object. The scale-axis transformation by Giesen et al. [65] and Miklos et al. [119] fails to guarantee that the skeleton is included in the original object. An alternative definition of scale axis transform introduced by Postolski et al. [143] guarantees the inclusion of the skeleton.

In digital approaches of skeletonization, skeletal pruning strategies have been adopted to control the trade-off between the simplicity of the skeleton and the inclusion of important object features. Borgefors et al. [35] presented a multi-scale discrete skeletonization algorithm generating multi-resolution decomposition and hierarchical skeletal representation of objects. Several researchers have used a global shape significance factor [7,12,81,163] and a predefined threshold of this factor to distinguish relevant skeletal branches carrying important object information from those generated by small scale protruding dents on object boundaries. The advantage of the global shape significance factor is that it ignores the section of a branch that grows only for connectedness preservation while capturing the section carrying geometric object information. Attali et al. [12] laid down the foundation of global significance measures of skeletal branches which was further generalized and improved by others [7,12,81,163]. Németh et al. [126] have recommended an iteration-by-iteration smoothing approach to improve the quality of final skeletons.

6. Applications

Skeletonization has been popularly used in many image processing and computer vision applications, including shape recognition and analysis, shape decomposition, character recognition, fingerprint analysis, animation, motion tracking, registration, interpolation, path-tracking, medical imaging applications etc. In the following, we list only a few examples. Thibault and Gold [187] applied Voronoi skeletonization algorithms to construct terrain models of valleys and ridges and their topological relationships from contour data. Gagvani and Silver [61] applied multi-scale skeletonization to construct a compact volumetric model of a 3-D object and used the model to reconstruct volumetric expressions under different animation poses and motions. Wade and Parent [192] used a skeletal path-tree and path-smoothing to generate a 3-D model from a volumetric object and applied it for animation. da Fontoura Costa and Cesar [51] discussed the usefulness of skeletal points together with their distance to the object boundary in object animation, smoothing, and matching. Several researchers have used skeletonization for data compression [78,97].

Sundar et al. [182] developed an algorithm for shape matching and retrieval using the geometric and topological information embedded in skeletal graphs. Brennecke and Isenberg [37] used skeletal graphs for 3-D shape matching. Aslan et al. [9] presented a new skeletal representation and demonstrated its effectiveness in addressing various challenges of deformable shape recognition. Bai and Latecki [13] introduced a new skeletal graph matching algorithm by comparing the geodesic paths between skeleton endpoints to develop a robust shape recognition algorithm based on object silhouettes. Cornea et al. [48] reviewed several applications of curve skeletonization including computer graphics, virtual navigation, segmentation, quantification, registration, matching, morphing, object decomposition, etc. Fujiyoshi et al. [60] applied skeletonization to track human motion in a video stream.

Skeletonization has been widely used for off-line character recognition [1,8,55,93] and fingerprint analysis [56,70,146,201]. Skeletonization has been popularly used for decomposition of shapes into meaningful segments [46,49,114,147,158,169]. Malandain et al. [114] and Saha and Chaudhuri [158] presented algorithms to automatically detect topological classes (e.g., surface or curve interiors, edges, or junctions) of individual voxels of a surface skeleton and formulated an "unglue" operation to separate different topological segments in a surface skeleton. Others have used curve skeletons and combined both geometric and topologic features to decompose different segments in a volumetric shape [46,49,147,169]. Recently, Serino et al. [169] have presented an object decomposition method achieved through skeleton decomposition. The skeleton is polygonally approximated, taking into account spatial position and distance values of its voxels, by segments along which no significant curvature changes occur and distance values are either constant or linearly changing. Each segment is interpreted as the spine of a simple part.

Skeletonization has been widely used in different medical imaging applications. Among these applications, two popular areas

are – (1) tracking and analysis of elongated anatomic structures and (2) quantitative characterization of anatomic object morphology.

Centerline approaches have been widely applied in arterial and vascular imaging, stenosis detection, colonoscopy, bronchoscopy, pulmonary imaging, etc. Tom et al. [188] applied skeletonization to determine the correspondence among skeletal pixels in two consecutive angiographic image frames using a dynamic programming-based approach. Kim et al. [83] used skeletal bifurcations as landmarks to compute local deformations between two consecutive image frames. Yim et al. [200] designed a gray-scale skeletonization method to interactively detect small vessel paths and for determination of branching patterns of vascular trees. Fridman et al. [57] used skeletonization for computation of cores to extract blood vessel trees in MR angiogram data. Selle et al. [168] applied skeletonization to assess the structural properties of the hepatic vessels and their relationship with tumors for liver surgical planning.

Skeletonization has become an essential step in stenosis detection [45,71,166,178–180,199], where vessel diameters are analyzed along the centerline and sudden depressions in diameter values along the centerline are detected as locations of stenosis. Nyström and Smedby [127] applied distance transform and centerline analysis techniques to generate enhanced visualization of stenoses in MR angiography.

Centerline detection has been popularly used for automated path finding in virtual colonoscopy [58,75,82,153,193] and bronchoscopy [86,121]. Using curve skeletonization on in vivo CT imaging, Tschirren et al. [191] developed a method for automated matching of corresponding branch points between two human airway trees, as well as for assigning anatomical names or labels to different branch segments of the human airway tree. Chaturvedi and Lee [42] applied skeletonization for airway tree analysis in micro-CT lung imaging for small animals. Also, curve skeletonization has been applied on other applications of pulmonary imaging [109,136] and tree analysis in surgical planning [168].

Another popular area of application of skeletonization in medical imaging is the quantitative characterization of object morphology, where a skeleton is used as a compact representation of the object. Kobatake and Yoshinaga [87] applied Hough transform to detect radiating line structures on skeletons, which are used to locate spicules on mammograms for malignant tumor identification. Zwiggelaar et al. [202] used skeletonization for detecting linear structures in mammograms, and for classifying those into different anatomical types, e.g., vessels, spicules, ducts, etc. Näf et al. [125] applied 3-D Voronoi skeletonization for characterization and recognition of complex anatomic shapes.

Saha and his colleagues developed digital topological analysis [157,158] of surface skeletons [160], which has been popularly applied to characterize trabecular bone as plate or rod micro-architecture to assess bone strength from in vivo imaging [41,67,90,99,181,196]. Recently, they further generalized to theory to characterize individual trabeculae on the continuum between a perfect plate and a perfect rod [163]. Others have used skeletonization as the first step to assess trabecular bone thickness, spacing and various network properties [76,91,138,144].

Besides the above two major areas, Pizer et al. [140] demonstrated applications of the skeleton-based model of the object shape in medical image segmentation and registration. Chatzis and Pitas [44] demonstrated an application of skeletonization in image interpolation, where skeletons on two adjacent images slices are used to build their correspondence and to compute the regional transformation field for interpolation.

7. Performance evaluation

Performance evaluation of a skeletonization algorithm is a serious research challenge emerging from the lack of definition of the

"true" skeleton for a digital object. Therefore, a widely accepted approach evaluating the performance of a skeletonization algorithm is yet absent in the literature. Different research groups have adopted different paths to evaluate the performance of their algorithms. Early skeletonization algorithms [4,92,190] were qualitatively evaluated through illustrations of results of example digital shapes. Haralick [73] discussed the guidelines for evaluating skeletonization algorithms and outlined some criteria of an error function for quantitative performance analysis. Jaisimha et al. [79] evaluated 2-D skeletonization algorithms in terms of robustness under added noise. Saha et al. [160] evaluated 3-D skeletonization in terms of robustness under border noise and image rotation. Sanniti di Baja [165] and Arcelli et al. [7] recommended the performance criterion of a skeletonization algorithm as the accuracy of the reconstruction of the original object from its skeleton. However, such criteria remains blind to the performance of an algorithm in terms of the quality of the shape of the skeleton and also ignore the sensitivity of an algorithm under noise, rotation, and repeat scan data acquisition. The Rotterdam coronary axis tracking evaluation group [166] reported results of a comprehensive evaluation study for centerline detection algorithms for coronary vasculature using consensus centerline with multiple observers and different quantitative measures of accuracy on a database containing 32 cardiac CTA datasets. Greenspan et al. [71] reported an evaluation study for center-line extraction algorithms in quantitative coronary angiography using a simulated coronary artery with known centerline and diameter function. Recently, Jin and Saha [81] reported a framework starting from a known skeleton and constructing corresponding objects at different conditions of imaging artifacts of noise and image resolution. Recently, Sobiecki et al. [177,176] have reported the results of performance evaluating studies for curve and surface skeletonization algorithms in voxel grids.

In general, the above performance evaluation frameworks report an error defined as some measure of disagreement between the expected and the computed skeletons. A concern with such approaches is that the average measure of errors does not reflect the performance of an algorithm in terms of generating spurious branches, missing true branches, preserving sharp corners, or digital smoothness over a contiguous surface or curve under different conditions of noise, resolution, and rotation. A comprehensive and consensus framework for evaluating skeletonization algorithms providing structured knowledge of understanding of their performance under various categories at different imaging conditions is yet to emerge. However, based on the principle used in a skeletonization algorithm, one may anticipate its expected behavior which may be useful in selecting an appropriate category of skeletonization algorithm for a specific application. Obviously, parallel skeletonization algorithms have the added advantage in terms of computational efficiency. At the same time, such algorithms face additional challenges in maintaining the expected geometry of the skeleton due to the asynchronous sequence of simple point removal. DT-based approaches are expected to show a better performance under rotation and at sharp corners due to the underlying robust strategy of using the DT, or depth measure, in defining the peel sequence. However, it is difficult to make such a distinction between DT-based and iterative skeletonization algorithms in terms of performance under noise. In the context of eliminating noisy branches, an algorithm based on assessment of the global significance of a branch is expected to be superior as compared to local decision based approaches during peeling. A comprehensive and consensus framework for evaluating the performance of skeletonization algorithms for various conditions will be helpful in selecting the right skeletonization algorithm for a given application.

8. Conclusion

A large number of computational approaches have been published for extracting the skeleton of an object, some of which are widely

different in terms of their principles. Significant research efforts have been dedicated toward enhancing the performance of skeletonization algorithms in terms of noisy branches, sharpness at corners, invariance under image transformation, reconstruction of original objects, etc. Skeletonization has been widely applied in various applications, especially in biomedical imaging, including pulmonary, cardiac, mammographic, abdominal, retinal, bone imaging, etc. Validation of skeletonization algorithms is a challenging issue and a comprehensive and consensus framework for evaluation is yet to emerge.

References

[1] M. Ahmed, R. Ward, A rotation invariant rule-based thinning algorithm for character recognition, IEEE Trans. Pattern Anal. Mach. Intell. 24 (2002) 1672–1678.

[2] N. Ahuja, J.-H. Chuang, Shape representation using a generalized potential field model, IEEE Trans. Pattern Anal. Mach. Intell. 19 (1997) 169–176.

[3] N. Amenta, S. Choi, R.K. Kolluri, The power crust, unions of balls, and the medial axis transform, Comput. Geom.: Theory Appl. 19 (2001) 127–153.

[4] C. Arcelli, G. Sanniti di Baja, A width-independent fast thinning algorithm, IEEE Trans. Pattern Anal. Mach. Intell. 7 (1985) 463–474.

[5] C. Arcelli, G. Sanniti di Baja, Finding local maxima in a pseudo-euclidean distance transform, Comput. Vis. Graph. Image Process. 43 (1988) 361–367.

[6] C. Arcelli, G. Sanniti di Baja, L. Serino, A parallel algorithm to skeletonize the distance transform of 3D objects, Image Vis. Comput. 27 (2009) 666–672.

[7] C. Arcelli, G. Sanniti di Baja, L. Serino, Distance-driven skeletonization in voxel images, IEEE Trans. Pattern Anal. Mach. Intell. 33 (2011) 709–720.

[8] N. Arica, F.T. Yarman-Vural, An overview of character recognition focused on off-line handwriting, IEEE Trans. Syst. Man Cybern. Part C: Appl. Rev. 31 (2001) 216–233.

[9] C. Aslan, A. Erdem, E. Erdem, S. Tari, Disconnected skeleton: shape at its absolute scale, IEEE Trans. Pattern Anal. Mach. Intell. 30 (2008) 2188–2203.

[10] D. Attali, J.-D. Boissonnat, H. Edelsbrunner, Stability and computation of medial axes-a state-of-the-art report, in: T. Möller, B. Hamann, R. Russell (Eds.), Mathematical Foundations of Scientific Visualization, Computer Graphics, and Massive Data Exploration, Springer-Verlag, Berlin, Germany, 2009, pp. 109–125.

[11] D. Attali, A. Montanvert, Computing and simplifying 2D and 3D continuous skeletons, Comput. Vis. Image Und. 67 (1997) 261–273.

[12] D. Attali, G. Sanniti di Baja, E. Thiel, Skeleton simplification through non significant branch removal, Image Process. Commun. 3 (1997) 63–72.

[13] X. Bai, L.J. Latecki, Path similarity skeleton graph matching, IEEE Trans. Pattern Anal. Mach. Intell. 30 (2008) 1282–1292.

[14] X. Bai, L.J. Latecki, W.Y. Liu, Skeleton pruning by contour partitioning with discrete curve evolution, IEEE Trans. Pattern Anal. Mach. Intell. 29 (2007) 449–462.

[15] G. Bertrand, On P-simple points, Comp. Rend. Acad. Sci. Paris (Comput. Sci./Theory Signals), Sér. Math. 1 321 (1995) 1077–1084.

[16] G. Bertrand, P-simple points: a solution for parallel thinning, in: Proceedings of the 5th International Conference on Discrete Geometry, France, 1995, pp. 233–242.

[17] G. Bertrand, A parallel thinning algorithm for medial surfaces, Pattern Recognit. Lett. 16 (1995) 979–986.

[18] G. Bertrand, Z. Aktouf, Three-dimensional thinning algorithm using subfields, in: Proceedings of the International Conference on Visual Geometry, SPIE, Boston, MA, 1995, pp. 113–124.

[19] G. Bertrand, M. Couprie, A new 3D parallel thinning scheme based on critical kernels, Discrete Geometry for Computer Imagery, Springer, France, 2006, pp. 580–591.

[20] G. Bertrand, M. Couprie, Two-dimensional parallel thinning algorithms based on critical kernels, J. Math. Imag. Vis. 31 (2008) 35–56.

[21] G. Bertrand, M. Couprie, On parallel thinning algorithms: minimal non-simple sets, P-simple points and critical kernels, J. Math. Imag. Vis. 35 (2009) 23–35.

[22] G. Bertrand, G. Malandain, A new characterization of three-dimensional simple points, Pattern Recognit. Lett. 15 (1994) 169–175.

[23] I. Bitter, A.E. Kaufman, M. Sato, Penalized-distance volumetric skeleton algorithm, IEEE Trans. Vis. Comput. Graph. 7 (2001) 195–206.

[24] H. Blum, A transformation for extracting new descriptors of shape, Models Percept. Speech Vis. Form 19 (1967) 362–380.

[25] H. Blum, R. Nagel, Shape description using weighted symmetric axis features, Pattern Recognit. 10 (1978) 167–180.

[26] G. Borgefors, Distance transform in arbitrary dimensions, Comput. Vis. Graph. Imag. Process. 27 (1984) 321–345.

[27] G. Borgefors, Distance transformations in digital images, Comput. Vis. Graph. Imag. Process. 34 (1986) 344–371.

[28] G. Borgefors, Centres of maximal discs in the 5-7-11 distance transform, in: Proceedings of the Scandinavian Conference on Image Analysis. Proceedings Published by Various Publishers, 1993, p. 105.

[29] G. Borgefors, On digital distance transformation in three dimensions, Comput. Vis. Graph. Imag. Process. 64 (1996) 368–376.

[30] G. Borgefors, Weighted digital distance transforms in four dimensions, Discrete Appl. Math. 125 (2003) 161–176.

[31] G. Borgefors, I. Nyström, Efficient shape representation by minimizing the set of centres of maximal discs/spheres, Pattern Recognit. Lett. 18 (1997) 465–471.

[32] G. Borgefors, I. Nyström, G. Sanniti di Baja, Surface skeletonization of volume objects, in: P. Perner, P. Wang, A. Rosenfeld (Eds.), Int. Work Adv. Struct. Syntac Pattern Recogntion, Leipzig, Germany, 1996, pp. 251–259.

[33] G. Borgefors, I. Nyström, G. Sanniti di Baja, Computing skeletons in three dimensions, Pattern Recognit. 32 (1999) 1225–1236.

[34] G. Borgefors, I. Nyström, G. Sanniti di Baja, S. Svensson, Simplification of 3D skeletons using distance information, in: International Conference on Vision Geometry, San Diego, CA, 2000, pp. 300–309.

[35] G. Borgefors, G. Ramella, G. Sanniti di Baja, Hierarchical decomposition of multiscale skeletons, IEEE Trans. Pattern Anal. Mach. Intell. 23 (2001) 1296–1312.

[36] J.W. Brandt, V.R. Algazi, Continuous skeleton computation by Voronoi diagram, CVGIP: Imag. Und. 55 (1992) 329–338.

[37] A. Brennecke, T. Isenberg, 3D shape matching using skeleton graphs, in: Proceedings of the Simulation and Visualization, Citeseer, 2004, pp. 299–310.

[38] A. Bucksch, R. Lindenbergh, CAMPINO—a skeletonization method for point cloud processing, ISPRS J. Photogram. Remote Sens. 63 (2008) 115–127.

[39] J. Burguet, R. Malgouyres, Strong thinning and polyhedric approximation of the surface of a voxel object, Discrete Appl. Math. 125 (2003) 93–114.

[40] M.J. Cardoso, M.J. Clarkson, M. Modat, S. Ourselin, On the extraction of topologically correct thickness measurements using Khalimsky's cubic complex, in: G. Székely, H.K. Hahn (Eds.), Information Processing in Medical Imaging (IPMI), Springer, 2011, pp. 159–170.

[41] G. Chang, S.K. Pakin, M.E. Schweitzer, P.K. Saha, R.R. Regatte, Adaptations in trabecular bone microarchitecture in Olympic athletes determined by 7T MRI, J. Magn. Reson. Imaging 27 (2008) 1089–1095.

[42] A. Chaturvedi, Z. Lee, Three-dimensional segmentation and skeletonization to build an airway tree data structure for small animals, Phys. Med. Biol. 50 (2005) 1405.

[43] V. Chatzis, I. Pitas, A generalized fuzzy mathematical morphology and its application in robust 2-D and 3-D object representation, IEEE Trans. Imag. Process. 9 (2000) 1798–1810.

[44] V. Chatzis, I. Pitas, Interpolation of 3-D binary images based on morphological skeletonization, IEEE Trans. Med. Imag. 19 (2000) 699–710.

[45] S.Y. Chen, J.D. Carroll, J.C. Messenger, Quantitative analysis of reconstructed 3-D coronary arterial tree and intracoronary devices, IEEE Trans. Med. Imag. 21 (2002) 724–740.

[46] P.-Y. Chiang, C.-C.J. Kuo, Voxel-based shape decomposition for feature-preserving 3D thumbnail creation, J. Vis. Commun. Image Reprod. 23 (2012) 1–11.

[47] Y. Cointepas, I. Bloch, L. Garnero, A cellular model for multi-objects multidimensional homotopic deformations, Pattern Recognit. 34 (2001) 1785–1798.

[48] N.D. Cornea, D. Silver, P. Min, Curve-skeleton properties, applications, and algorithms, IEEE Trans. Vis. Comput. Graph. 13 (2007) 530–548.

[49] N.D. Cornea, D. Silver, X. Yuan, R. Balasubramanian, Computing hierarchical curve-skeletons of 3D objects, Vis. Comput. 21 (2005) 945–955.

[50] M. Couprie, Topological maps and robust hierarchical Euclidean skeletons in cubical complexes, Comput. Vis. Image Und. 117 (2013) 355–369.

[51] L da Fontoura Costa, R.M. Cesar Jr., Shape Analysis and Classification: Theory and Practice, CRC Press, 2000.

[52] T.K. Dey, W. Zhao, Approximating the medial axis from the Voronoi diagram with a convergence guarantee, Algorithmica 38 (2004) 179–200.

[53] A.R. Dill, M.D. Levine, P.B. Noble, Multiple resolution skeletons, IEEE Trans. Pattern Anal. Mach. Intell. (1987) 495–504.

[54] P. Dlotko, R. Specogna, Topology preserving thinning of cell complexes, IEEE Trans. Image Process. 23 (2014) 4486–4495.

[55] Ø. Due Trier, A.K. Jain, T. Taxt, Feature extraction methods for character recognition-a survey, Pattern Recognit. 29 (1996) 641–662.

[56] A. Farina, Z.M. Kovacs-Vajna, A. Leone, Fingerprint minutiae extraction from skeletonized binary images, Pattern Recognit. 32 (1999) 877–889.

[57] Y. Fridman, S.M. Pizer, S. Aylward, E. Bullitt, Extracting branching tubular object geometry via cores, Med. Image Anal. 8 (2004) 169–176.

[58] H. Frimmel, J. Näppi, H. Yoshida, Centerline-based colon segmentation for CT colonography, Med. Phys. 32 (2005) 2665–2672.

[59] D.S. Fritsch, S.M. Pizer, B.S. Morse, D.H. Eberly, A. Liu, The multiscale medial axis and its applications in image registration, Pattern Recognit. Lett. 15 (1994) 445–452.

[60] H. Fujiyoshi, A.J. Lipton, T. Kanade, Real-time human motion analysis by image skeletonization, IEICE Trans. Inf. Syst. 87 (2004) 113–120.

[61] N. Gagvani, D. Silver, Animating volumetric models, Graph Mod. 63 (2001) 443–458.

[62] C.-J. Gau, T.Y. Kong, Minimal nonsimple sets of voxels in binary images on a face-centered cubic grid, Int. J. Pattern Recognit. Artif. Intell. 13 (1999) 485–502.

[63] C.-J. Gau, T.Y. Kong, Minimal non-simple sets in 4D binary images, Graph Mod. 65 (2003) 112–130.

[64] P.J. Giblin, B.B. Kimia, A formal classification of 3D medial axis points and their local geometry, IEEE Trans. Pattern Anal. Mach. Intell., 26 (2004) 238–251.

[65] J. Giesen, B. Miklos, M. Pauly, C. Wormser, The scale axis transform, in: Proceedings of the 25th Annual Symposium on Computational Geometry, ACM, 2009, pp. 106–115.

[66] M.J. Golay, Hexagonal parallel pattern transformations, IEEE Trans. Comput. 18 (1969) 733–740.

[67] B.G. Gomberg, P.K. Saha, H.K. Song, S.N. Hwang, F.W. Wehrli, Topological analysis of trabecular bone MR images, IEEE Trans. Med. Imaging 19 (2000) 166–174.

[68] W. Gong, G. Bertrand, A simple parallel 3D thinning algorithm, in: Proceedings of the 10th IEEE International Conference on Pattern Recognition, 1990, pp. 188–190.

[69] L. Gorelick, M. Galun, E. Sharon, R. Basri, A. Brandt, Shape representation and classification using the Poisson equation, IEEE Trans. Pattern Anal. Mach. Intell. 28 (2006) 1991–2005.

[70] S. Greenberg, M. Aladjem, D. Kogan, I. Dimitrov, Fingerprint image enhancement using filtering techniques, in: Proceedings of the IEEE International Conference on Pattern Recognition, Barcelona, Spain, 2000, pp. 322–325.

[71] H. Greenspan, M. Laifenfeld, S. Einav, O. Barnea, Evaluation of center-line extraction algorithms in quantitative coronary angiography, IEEE Trans. Med. Imaging, 20 (2001) 928–941.

[72] R.W. Hall, Tests for connectivity preservation for parallel reduction operators, Topol. Appl. 46 (1992) 199–217.

[73] R.M. Haralick, Performance characterization in image analysis: thinning, a case in point, Pattern Recognit. Lett. 13 (1992) 5–12.

[74] M.S. Hassouna, A.A. Farag, Variational curve skeletons using gradient vector flow, IEEE Trans. Pattern Anal. Mach. Intell. 31 (2009) 2257–2274.

[75] T. He, L. Hong, D. Chen, Z. Liang, Reliable path for virtual endoscopy: ensuring complete examination of human organs, IEEE Trans. Vis. Comput. Graph. 7 (2001) 333–342.

[76] T. Hildebrand, P. Rüegsegger, A new method for the model independent assessment of thickness in three-dimensional images, J. Microsc. 185 (1997) 67–75.

[77] C.J. Hilditch, Linear skeletons from square cupboards, in: B. Meltzer, D. Michie (Eds.), Machine Intelligence, Edinburgh University Press, Edinburgh, U.K., 1969, pp. 403–420.

[78] L. Huang, A. Bijaoui, Astronomical image data compression by morphological skeleton transformation, Exp. Astron. 1 (1990) 311–327.

[79] M.Y. Jaisimha, R.M. Haralick, D. Dori, Quantitative performance evaluation of thinning algorithms under noisy conditions, in: Proceedings of the International Conference on Computer Vision and Pattern Recognition, Seattle, WA, 1994, pp. 678–683.

[80] A.C. Jalba, J. Kustra, A.C. Telea, Surface and curve skeletonization of large 3D models on the GPU, IEEE Trans. Pattern Anal. Mach. Intell., 35 (2013) 1495–1508.

[81] D. Jin, P.K. Saha, A new fuzzy skeletonization algorithm and its applications to medical imaging, in: Proceedings of the 17th Internationl Conference on Image Analysis and Processing, Naples, Italy, 2013, pp. 662–671.

[82] D.G. Kang, J.B. Ra, A new path planning algorithm for maximizing visibility in computed tomography colonography, IEEE Trans. Med. Imaging 24 (2005) 957–968.

[83] H.C. Kim, B.G. Min, M.K. Lee, J.D. Seo, Y.W. Lee, M.C. Han, Estimation of local cardiac wall deformation and regional wall stress from biplane coronary cineangiograms, IEEE Trans. Biomed. Eng. 32 (1985) 503–512.

[84] B.B. Kimia, A. Tannenbaum, S.W. Zucker, Shape, shocks, and deformations. I. The components of two-dimensional shape and the reaction-diffusion space, Int. J. Comp. Vis. 15 (1995) 189–224.

[85] R. Kimmel, D. Shaked, N. Kiryati, Skeletonization via distance maps and level sets, Comput. Vis. Image Process. 62 (1995) 382–391.

[86] A.P. Kiraly, J.P. Helferty, E.A. Hoffman, G. McLennan, W.E. Higgins, Three-dimensional path planning for virtual bronchoscopy, IEEE Trans. Med. Imaging 23 (2004) 1365–1379.

[87] H. Kobatake, Y. Yoshinaga, Detection of spicules on mammogram based on skeleton analysis, IEEE Trans. Med. Imaging 15 (1996) 235–245.

[88] T.Y. Kong, Topology-preserving deletion of 1's from 2-, 3-and 4-dimensional binary images, in: Proceedings of the International Workshop on Discrete Geometry for Computer Imagery, Montpellier, France, Springer, 1997, pp. 1–18.

[89] T.Y. Kong, Minimal non-deletable sets and minimal non-codeletable sets in binary images, Theor. Comput. Sci. 406 (2008) 97–118.

[90] G.A. Ladinsky, B. Vasilic, A.M. Popescu, M. Wald, B.S. Zemel, P.J. Snyder, L. Loh, H.K. Song, P.K. Saha, A.C. Wright, F.W. Wehrli, Trabecular structure quantified with the MRI-based virtual bone biopsy in postmenopausal women contributes to vertebral deformity burden independent of areal vertebral BMD, J. Bone Min. Res. 23 (2008) 64–74.

[91] A. Laib, D.C. Newitt, Y. Lu, S. Majumdar, New model-independent measures of trabecular bone structure applied to in vivo high-resolution MR images, Osteopor. Int. 13 (2002) 130–136.

[92] L. Lam, S.-W. Lee, C.Y. Suen, Thinning methodologies – a comprehensive survey, IEEE Trans. Pattern Anal. Mach. Intell. 14 (1992) 869–885.

[93] L. Lam, C.Y. Suen, An evaluation of parallel thinning algorithms for character recognition, IEEE Trans. Pattern Anal. Mach. Intell. 17 (1995) 914–919.

[94] C. Lantuejoul, Skeletonization in Quantitative Metallography, Issues of Digital Image Processing, Sijthoff and Noordhoff, Groningen, The Netherlands, 1980.

[95] T.-C. Lee, R.L. Kashyap, C.-N. Chu, Building skeleton models via 3-D medial surface/axis thinning algorithm, CVGIP: Graph. Mod. Image Process. 56 (1994) 462–478.

[96] F. Leymarie, M.D. Levine, Simulating the grassfire transform using an active contour model, IEEE Trans. Pattern Anal. Mach. Intell. 14 (1992) 56–75.

[97] J.-M. Lien, G. Kurillo, R. Bajcsy, Skeleton-based data compression for multi-camera tele-immersion system, Advances in Visual Computing, Springer, 2007, pp. 714–723.

[98] L. Liu, E.W. Chambers, D. Letscher, T. Ju, A simple and robust thinning algorithm on cell complexes, Computer Graphics Forum, Wiley Online Library, 2010, pp. 2253–2260.

[99] X.S. Liu, P. Sajda, P.K. Saha, F.W. Wehrli, G. Bevill, T.M. Keaveny, X.E. Guo, Complete volumetric decomposition of individual trabecular plates and rods and its morphological correlations with anisotropic elastic moduli in human trabecular bone, J. Bone Min. Res., 23 (2008) 223–235.

[100] S. Lobregt, P.W. Verbeek, F.C.A. Groen, Three-dimensional skeletonization, principle, and algorithm, IEEE Trans. PattERN Anal. Mach. Intell. 2 (1980) 75–77.

[101] C. Lohou, Detection of the non-topology preservation of Ma's 3D surface-thinning algorithm, by the use of P-simple points, Pattern Recognit. Lett. 29 (2008) 822–827.

[102] C. Lohou, Detection of the non-topology preservation of Ma and Sonka's algorithm, by the use of P-simple points, Comput. Vis. Image Und. 114 (2010) 384–399.

[103] C. Lohou, G. Bertrand, A 3D 12-subiteration thinning algorithm based on P-simple points, Discrete Appl. Math. 139 (2004) 171–195.

[104] C. Lohou, G. Bertrand, A 3D 6-subiteration curve thinning algorithm based on P-simple points, Discrete Appl. Math. 151 (2005) 198–228.

[105] C. Lohou, G. Bertrand, Two symmetrical thinning algorithms for 3D binary images, based on P-simple points, Pattern Recognit. 40 (2007) 2301–2314.

[106] C. Lohou, J. Dehos, Automatic correction of Ma and Sonka's thinning algorithm using P-simple points, IEEE Trans. Pattern Anal. Mach. Intell. 32 (2010) 1148–1152.

[107] C.M. Ma, On topology preservation in 3D thinning, CVGIP: Image Und. 59 (1994) 328–339.

[108] C.M. Ma, Connectivity preservation of 3D 6-subiteration thinning algorithms, Graph Mod. Image Process. 58 (1996) 382–386.

[109] C.M. Ma, M. Sonka, A fully parallel 3D thinning algorithm and its applications, Comput. Vis. Image Und. 64 (1996) 420–433.

[110] C.M. Ma, S.Y. Wan, Parallel thinning algorithms on 3D (18, 6) binary images, Comput. Vis. Image Und. 80 (2000) 364–378.

[111] C.M. Ma, S.Y. Wan, J.D. Lee, Three-dimensional topology preserving reduction on the 4-subfields, IEEE Trans. Pattern Anal. Mach. Intell. 24 (2002) 1594–1605.

[112] J. Ma, S.W. Bae, S. Choi, 3D medial axis point approximation using nearest neighbors and the normal field, Vis. Comput. 28 (2012) 7–19.

[113] G. Malandain, G. Bertrand, Fast characterization of 3-D simple points, in: Proceedings of the 11th International Conference on Pattern Recognition, 1992, pp. 232–235.

[114] G. Malandain, G. Bertrand, N. Ayache, Topological segmentation of discrete surfaces, Int. J. Comput. Vis. 10 (1993) 183–197.

[115] R. Malgouyres, S. Fourey, Strong surfaces, surface skeletons, and image superimposition, International Conference on Visualization Geometry, SPIE, San Diego, CA, 1998, pp. 16–27.

[116] P.A. Maragos, R.W. Schafer, Morphological skeleton representation and coding of binary images, IEEE Trans. Acoustics Speech Signal Process. 34 (1986) 228–244.

[117] G. Matheron, Random Sets and Integral Geometry, John Wiley & Sons, New York, 1975.

[118] G. Matheron, Examples of topological properties of skeletons, in: J. Serra (Ed.), Image Analysis and Mathematical Morphology, Part II: Theoretical Advances, 1988, pp. 217–238.

[119] B. Miklos, J. Giesen, M. Pauly, Discrete scale axis representations for 3D geometry, ACM Trans Graph 29 (2010) 101.

[120] D.G. Morgenthaler, Three-dimensional simple points: serial erosion, parallel thinning and skeletonization, Computer Vision Laboratory, University of Maryland, College Park, MD, 1981 TR-1005.

[121] K. Mori, J. Hasegawa, Y. Suenaga, J. Toriwaki, Automated anatomical labeling of the bronchial branch and its application to the virtual bronchoscopy system, IEEE Trans. Med. Imaging 19 (2000) 103–114.

[122] B.S. Morse, S.M. Pizer, A. Liu, Multiscale medial analysis of medical images, in: Proceedings of the International Conference on Information Processing and Medical Imaging, Springer, 1993, pp. 112–131.

[123] J. Mukherjee, P.P. Das, B. Chatterji, On connectivity issues of ESPTA, Pattern Recognit. Lett. 11 (1990) 643–648.

[124] J. Mylopoulos, T. Pavlidis, On the topological properties of quantized spaces. II. Connectivity and order of connectivity, J. Assoc. Comput. Mach. 18 (1971) 247–254.

[125] M. Näf, G. Székely, R. Kikinis, M.E. Shenton, O. Kübler, 3D voronoi skeletons and their usage for the characterization and recognition of 3D organ shape, Comput. Vis. Image Und. 66 (1997) 147–161.

[126] G. Németh, P. Kardos, K. Palágyi, Thinning combined with iteration-by-iteration smoothing for 3D binary images, Graph Mod. 73 (2011) 335–345.

[127] I. Nyström, Ö. Smedby, Skeletonization of volumetric vascular images—distance information utilized for visualization, J. Combinat. Optim. 5 (2001) 27–41.

[128] R. Ogniewicz, M. Ilg, Voronoi skeletons: theory and applications, in: Proceedings of the IEEE International Conference on Computer Vision and Pattern Recognition, 1992, pp. 63–69.

[129] R.L. Ogniewicz, O. Kübler, Hierarchic voronoi skeletons, Pattern Recognit. 28 (1995) 343–359.

[130] K. Palágyi, A 3-subiteration 3D thinning algorithm for extracting medial surfaces, Pattern Recognit. Lett. 23 (2002) 663–675.

[131] K. Palágyi, A 3D fully parallel surface-thinning algorithm, Theor. Comput. Sci. 406 (2008) 119–135.

[132] K. Palágyi, A. Kuba, A 3D 6-subiteration thinning algorithm for extracting medial lines, Pattern Recognit. Lett. 19 (1998) 613–627.

[133] K. Palágyi, A. Kuba, A hybrid thinning algorithm for 3D medical images, J. Comput. Inf. Technol. 6 (1998) 149–164.

[134] K. Palágyi, A. Kuba, Directional 3D thinning using 8 subiterations, in: G. Bertrand, M. Couprie, L. Perroton (Eds.), Proceedings of the International Conference on Discrete Geometry for Computer Imagery, Springer, 1999, pp. 325–336.

[135] K. Palágyi, A. Kuba, A parallel 3D 12-subiteration thinning algorithm, Graph Mod. Image Process. 61 (1999) 199–221.

[136] K. Palágyi, J. Tschirren, E.A. Hoffman, M. Sonka, Quantitative analysis of pulmonary airway tree structures, Comput. Biol. Med. 36 (2006) 974–996.

[137] N. Passat, M. Couprie, G. Bertrand, Minimal simple pairs in the 3-D cubic grid, J. Math. Image Vis. 32 (2008) 239–249.

[138] F. Peyrin, Z. Peter, A. Larrue, A. Bonnassie, D. Attali, Local geometrical analysis of 3D porous networks based on the medial axis: application to bone microarchitecture microtomography images, Image Anal. Stereol. 26 (2011) 179–185.

[139] S.M. Pizer, D. Eberly, D.S. Fritsch, B.S. Morse, Zoom-invariant vision of figural shape: the mathematics of core, Comput. Vis. Image Und. 69 (1998) 55–71.

[140] S.M. Pizer, D.S. Fritsch, P.A. Yushkevich, V.E. Johnson, E.L. Chaney, Segmentation, registration, and measurement of shape variation via image object shape, Med. Imaging, IEEE Trans. 18 (1999) 851–865.

[141] S.M. Pizer, W.R. Oliver, S.H. Bloomberg, Hierarchical shape description via the multiresolution symmetric axis transform, IEEE Trans. Pattern Anal. Mach. Intell. 9 (1987) 505–511.

[142] S.M. Pizer, K. Siddiqi, G. Székely, J.N. Damon, S.W. Zucker, Multiscale medial loci and their properties, Int. J. Comput. Vis. 55 (2003) 155–179.

[143] M. Postolski, M. Couprie, M. Janaszewski, Scale filtered Euclidean medial axis and its hierarchy, Comput. Vis. Image Und. 129 (2014) 89–102.

[144] L. Pothuaud, A. Laib, P. Levitz, C.L. Benhamou, S. Majumdar, Three-dimensional-line skeleton graph analysis of high-resolution magnetic resonance images: a validation study from 34-microm-resolution microcomputed tomography, J. Bone Min. Res. 17 (2002) 1883–1895.

[145] C. Pudney, Distance-ordered homotopic thinning: a skeletonization algorithm for 3D digital images, Comput. Vis. Image Und. 72 (1998) 404–413.

[146] M. Rao, T. Ch, Feature extraction for fingerprint classification, Pattern Recognit. 8 (1976) 181–192.

[147] D. Reniers, A. Telea, Skeleton-based hierarchical shape segmentation, in: Proceedings of the IEEE International Conference on Shape Modeling and Application, 2007, pp. 179–188.

[148] C. Ronse, A topological characterization of thinning, Theor. Comput. Sci. 43 (1986) 31–41.

[149] C. Ronse, Minimal test patterns for connectivity preservation in parallel thinning algorithms for binary digital images, Discrete Appl. Math. 21 (1988) 67–79.

[150] A. Rosenfeld, Connectivity in digital pictures, J. Assoc. Comput. Mach., 17 (1970) 146–160.

[151] A. Rosenfeld, Arcs and curves in digital pictures, J. Assoc. Comput. Mach., 20 (1973) 81–87.

[152] D. Rutovitz, Pattern recognition, J. Roy. Stat. Soc. 129 (1966) 504–530.

[153] R.J.T. Sadleir, P.F. Whelan, Fast colon centreline calculation using optimised 3D topological thinning, Comput. Med. Imaging Graph., 29 (2005) 251–258.

[154] P.K. Saha, 2D Thinning Algorithms and 3D Shrinking INRIA, Sophia Antipolis Cedex, France, 1991.

[155] P.K. Saha, B. Chanda, D.D. Majumder, Principles and Algorithms for 2-D and 3-D Shrinking, Indian Statistical Institute, Calcutta, India, 1991 TR/KBCS/2/91.

[156] P.K. Saha, B.B. Chaudhuri, Simple Point Computation and 3-D Thinning with Parallel Implementation, Indian Statistical Institute, Calcutta, India, 1993 TR/KBCS/1/93.

[157] P.K. Saha, B.B. Chaudhuri, Detection of 3-D simple points for topology preserving transformations with application to thinning, IEEE Trans. Pattern Anal. Mach. Intell. 16 (1994) 1028–1032.

[158] P.K. Saha, B.B. Chaudhuri, 3D digital topology under binary transformation with applications, Comput. Vis. Image Und. 63 (1996) 418–429.

[159] P.K. Saha, B.B. Chaudhuri, B. Chanda, D.D. Majumder, Topology preservation in 3D digital space, Pattern Recognit. 27 (1994) 295–300.

[160] P.K. Saha, B.B. Chaudhuri, D.D. Majumder, A new shape preserving parallel thinning algorithm for 3D digital images, Pattern Recognit. 30 (1997) 1939–1955.

[161] P.K. Saha, F.W. Wehrli, Fuzzy distance transform in general digital grids and its applications, in: Proceedings of the 7th Joint Conference on Information Sciences, Research Triangular Park, NC, 2003, pp. 201–213.

[162] P.K. Saha, F.W. Wehrli, B.R. Gomberg, Fuzzy distance transform: theory, algorithms, and applications, Comput. Vis. Image Und. 86 (2002) 171–190.

[163] P.K. Saha, Y. Xu, H. Duan, A. Heiner, G. Liang, Volumetric topological analysis: a novel approach for trabecular bone classification on the continuum between plates and rods, IEEE Trans. Med. Imaging 29 (2010) 1821–1838.

[164] T. Saito, J.-I. Toriwaki, A sequential thinning algorithm for three dimensional digital pictures using the Euclidean distance transformation, in: Proceedings of the 9th Scandinavian Conference on Image Analysis, Uppsala, Sweden, 1995, pp. 507–516.

[165] G Sanniti di Baja, Well-shaped, stable, and reversible skeletons from the (3,4)-distance transform, J. Vis. Commun. Image Reprod. 5 (1994) 107–115.

[166] M. Schaap, C.T. Metz, T. van Walsum, A.G. van der Giessen, A.C. Weustink, N.R. Mollet, C. Bauer, H. Bogunovic, C. Castro, X. Deng, E. Dikici, T. O'Donnell, M. Frenay, O. Friman, M. Hernandez Hoyos, P.H. Kitslaar, K. Krissian, C. Kuhnel, M.A. Luengo-Oroz, M. Orkisz, O. Smedby, M. Styner, A. Szymczak, H. Tek, C. Wang, S.K. Warfield, S. Zambal, Y. Zhang, G.P. Krestin, W.J. Niessen, Standardized evaluation methodology and reference database for evaluating coronary artery centerline extraction algorithms, Med. Image Anal. 13 (2009) 701–714.

[167] M. Schmitt, Some examples of algorithms analysis in computational geometry by means of mathematical morphological techniques, in: J.-D. Boissonnat, J.-P. Laumond (Eds.), Geometry and Robotics, Springer, Toulouse, France, 1989, pp. 225–246.

[168] D. Selle, B. Preim, A. Schenk, H.-O. Peitgen, Analysis of vasculature for liver surgical planning, IEEE Trans. Med. Imaging 21 (2002) 1344–1357.

[169] L. Serino, C. Arcelli, G. Sanniti di Baja, Decomposing 3D objects in simple parts characterized by rectilinear spines, Int. J. Pattern Recognit. Artif. Intell. 28 (2014) 1460010.1–19.

[170] J. Serra, Image Analysis and Mathematical Morphology, Academic Press, London, 1982.

[171] J. Shah, Extraction of shape skeletons from grayscale images, Comput. Vis. Image Und. 99 (2005) 96–109.

[172] E.C. Sherbrooke, N.M. Patrikalakis, E. Brisson, An algorithm for the medial axis transform of 3D polyhedral solids, IEEE Trans. Vis. Comput. Graph. 2 (1996) 44–61.

[173] K. Siddiqi, S. Bouix, A. Tannenbaum, S.W. Zucker, Hamilton-Jacobi Skeletons, Int. J. Comput. Vis. 48 (2002) 215–231.

[174] K. Siddiqi, B.B. Kimia, A shock grammar for recognition, in: Proceedings of the IEEE Conference on Computer Vision and Pattern Recognition, 1996, pp. 507–513.

[175] K. Siddiqi, S.M. Pizer, Medial Representations: Mathematics, Algorithms and Applications, Springer, 2008.

[176] A. Sobiecki, A. Jalba, A. Telea, Comparison of curve and surface skeletonization methods for voxel shapes, Pattern Recognit. Lett. 47 (2014) 147–156.

[177] A. Sobiecki, H.C. Yasan, A.C. Jalba, A.C. Telea, Qualitative comparison of contraction-based curve skeletonization methods, Mathematical Morphology and Its Applications to Signal and Image Processing, Springer, 2013, pp. 425–439.

[178] M. Sonka, M.D. Winniford, S.M. Collins, Robust simultaneous detection of coronary borders in complex images, IEEE Trans. Med. Imaging 14 (1995) 151–161.

[179] M. Sonka, M.D. Winniford, X. Zhang, S.M. Collins, Lumen centerline detection in complex coronary angiograms, IEEE Trans. Biomed. Eng. 41 (1994) 520–528.

[180] E. Sorantin, C. Halmai, B. Erdohelyi, K. Palagyi, L.G. Nyul, K. Olle, B. Geiger, F. Lindbichler, G. Friedrich, K. Kiesler, Spiral-CT-based assessment of tracheal stenoses using 3-D-skeletonization, IEEE Trans. Med. Imaging 21 (2002) 263–273.

[181] M. Stauber, R. Muller, Volumetric spatial decomposition of trabecular bone into rods and plates—a new method for local bone morphometry, Bone 38 (2006) 475–484.

[182] H. Sundar, D. Silver, N. Gagvani, S. Dickinson, Skeleton based shape matching and retrieval, in: Proc. Shape Model. Int., IEEE, Seoul, South Korea, 2003, pp. 130–139.

[183] S. Svensson, Aspects on the reverse fuzzy distance transform, Pattern Recognit. Lett. 29 (2008) 888–896.

[184] S. Svensson, G. Borgefors, I. Nyström, On reversible skeletonization using anchor-points from distance transforms, J. Vis. Commun. Image Reprod. 10 (1999) 379–397.

[185] G. Székely, Shape Characterization by Local Symmetries, Habilitation, Swiss Federal Institute of Technology, Zürich, 1996.

[186] Z.S.G. Tari, J. Shah, H. Pien, Extraction of shape skeletons from grayscale images, Comput. Vis. Image Und. 66 (1997) 133–146.

[187] D. Thibault, C.M. Gold, Terrain reconstruction from contours by skeleton construction, GeoInformatica 4 (2000) 349–373.

[188] B.S. Tom, S.N. Efstratiadis, A.K. Katsaggelos, Motion estimation of skeletonized angiographic images using elastic registration, IEEE Trans. Med. Imaging 13 (1994) 450–460.

[189] G. Tourlakis, J. Mylopoulos, Some results on computational topology, J. Assoc. Comput. Mach. 20 (1973) 439–455.

[190] Y.F. Tsao, K.S. Fu, A parallel thinning algorithm for 3D pictures, Comput. Graph. Image Process. 17 (1981) 315–331.

[191] J. Tschirren, G. McLennan, K. Palagyi, E.A. Hoffman, M. Sonka, Matching and anatomical labeling of human airway tree, IEEE Trans. Med. Imaging 24 (2005) 1540–1547.

[192] L. Wade, R.E. Parent, Automated generation of control skeletons for use in animation, Vis. Comput. 18 (2002) 97–110.

[193] M. Wan, Z. Liang, Q. Ke, L. Hong, I. Bitter, A. Kaufman, Automatic centerline extraction for virtual colonoscopy, IEEE Trans. Med. Imaging 21 (2002) 1450–1460.

[194] S. Wang, J. Wu, M. Wei, X. Ma, Robust curve skeleton extraction for vascular structures, Graph Mod. 74 (2012) 109–120.

[195] T. Wang, A. Basu, A note on 'A fully parallel 3D thinning algorithm and its applications', Pattern Recognit. Lett. 28 (2007) 501–506.

[196] F.W. Wehrli, B.R. Gomberg, P.K. Saha, H.K. Song, S.N. Hwang, P.J. Snyder, Digital topological analysis of in vivo magnetic resonance microimages of trabecular bone reveals structural implications of osteoporosis, J. Bone Min. Res. 16 (2001) 1520–1531.

[197] O. Wink, W.J. Niessen, M.A. Viergever, Multiscale vessel tracking, IEEE Trans. Med. Imaging 23 (2004) 130–133.

[198] W. Xie, R.P. Thompson, R. Perucchio, A topology-preserving parallel 3D thinning algorithm for extracting the curve skeleton, Pattern Recognit. 36 (2003) 1529–1544.

[199] Y. Xu, G. Liang, G. Hu, Y. Yang, J. Geng, P.K. Saha, Quantification of coronary arterial stenoses in CTA using fuzzy distance transform, Comput. Med. Imaging Graph. 36 (2012) 11–24.

[200] P.J. Yim, P.L. Choyke, R.M. Summers, Gray-scale skeletonization of small vessels in magnetic resonance angiography, IEEE Trans. Med. Imaging 19 (2000) 568–576.

[201] F. Zhao, X. Tang, Preprocessing and postprocessing for skeleton-based fingerprint minutiae extraction, Pattern Recognit. 40 (2007) 1270–1281.

[202] R. Zwiggelaar, S.M. Astley, C.R. Boggis, C.J. Taylor, Linear structures in mammographic images: detection and classification, IEEE Trans. Med. Imaging 23 (2004) 1077–1086.